EXPERIMENTAL STUDIES OF PHOTOCATHODE RF GUN WITH LASER PULSE SHAPING

J. Yang†, F. Sakai, T. Yanagida, M. Yorozu, Y. Okada, T. Nakajyo, Sumitomo Heavy Industries, Ltd., T2-1-1 Yatocho, Nishitokyo, Tokyo 188-8585, Japan
K. Takasago, A. Endo, Femtosecond Technology Research Association, 5-5 Tokodai, Tsukuba, Ibaraki 300-2635, Japan

Abstract

A technique of laser pulse shaping was developed for low-emittance electron beam generation in a photo-cathode RF gun. The emittance growth due to space charge and RF effects in the RF gun was experimentally investigated with square and gaussian temporal laser pulse shapes. It is found that the square pulse shaping is a useful tool for both the reduction of nonlinear space charge force and the correction of the linear space charge effect. An optimal normalized rms emittance of 1.2 πmm-mrad at 1 nC was obtained by a square temporal laser pulse shape with pulse length of 9 ps FWHM.

1 INTRODUCATION

The generation of a low-emittance electron beam is a key technology in free electron lasers[1], linear colliders[2] and laser Compton scatterings[3]. Typically, an electron beam with a normalized emittance of <1 πmm-mrad at 1 nC is desired in self-amplified spontaneous emission free electron laser in SLAC[1. To meet these requirements, laser-driven photocathode rf guns have been studied. The rf gun generates short electron bunches with short laser pulses. The electrons with a space charge induced emittance are emitted from the photocathode surface by a strong rf electric field.

However, the emittance growth in the rf gun occurs close to the cathode surface due to the defocusing space charge force, i.e. where the beam is not yet relativistic. The minimization of the defocusing space charge force is required in order to obtain the minimum expected emittance. Moreover, the reduction of nonlinear space charge effect is needed, because it causes a distortion to the phase space during acceleration and cannot be removed in the emittance compensation scheme. From theoretical studies [4,5], a technique of shaping temporal charge density distribution of electrons, i.e. a uniform temporal electron bunch, reduces the defocusing space charge force. It can be also tailed to behave like a linear space charge field, resulting in emittance compensation.

We report here on the first experimental observation of the beam transverse emittance growth in the rf gun with gaussian and square temporal laser pulse shaping. The beam transverse emittance measurements are made as functions of the laser pulse length and the electron charge.

†E-mail: jnf_yang@shi.co.jp

2 EXPERIMENTAL ARRANGEMENT

2.1 Photocathode RF Gun & Subsequent Linac

A S-band (2856 MHz) photocathode rf gun (BNL gun-IV [6,7]) was used for the electron generation. The rf gun was consisted of two cells: a half cell and a full cell. A copper cathode was located on the side of the half cell. The length of the half cell was designed to be 0.6 times of the full cell. At the exit of the rf gun, a solenoid magnet was mounted for space-charge emittance compensation.

The electron beam produced from the rf gun was accelerated with a 70 cm long standing-wave linear accelerator (linac) located downstream of the solenoid magnet at a position of 1.2 m from the cathode (see Fig. 1). The input rf peak power of both the rf gun and the linac was 7.5 MW that was produced with a 15 MW Klystron. The peak on-axis electric fields in the rf gun and the linac were 100 and 25 MV/m, respectively. The operating repetition rate was 10 Hz. The accelerated beam energy was 14 MeV (4 MeV at the gun exit). The beam energy spread was not measured in the experiments, but an optimal beam energy spread of 0.25% was measured downstream of the linac with a photo-cathode driven Nd:YAG laser with a pulse length of 11 ps FWHM[7].

To measure the beam transverse emittance, we used a standard quadrupole scan technique whereby the beam size was measured on a screen downstream of a quadrupole magnet which was varied so that the beam passed through a waist at the screen. The screen (100μm thick) was made of sintered Al_2O_3 doped with Cr. The beam images on the screen were acquired by a charge-coupled device (CCD) camera and a data translation 8-bit frame grabber synchronized to the electron beam. The image resolution achieved on the CCD camera was as small as 5μm/pixel. Each image of the beam profile captured from the screen was subtracted the image of a background shot with the rf on but the laser off. The subtracted background images were analysed off line and the beam profile was fitted to a gaussian distribution from which the rms beam size was obtained. The beam size at each quadrupole setting was measured by averaging 16 different images. The fluctuation of the beam size was 4-5%. The limitation on the beam size measurement was <68 μm using the beam imaging technique.

2.2 A photocathode-driving laser

A laser, used to drive the rf gun, was consisted of a femtosecond Ti:Sapphire laser oscillator, a temporal pulse shaper, a pulse stretcher, an amplifier, a pulse compressor and a frequency converter. The oscillator, which was passively mode-locked at a frequency of 119 MHz (the 24th sub-harmonic of the accelerating rf), generated a 50 fs long laser pulse with a central wavelength of 800 nm and a spectral width of 15 nm FWHM for pulse shaping.

The temporal pulse shaper was accomplished through a technique of frequency-domain pulse shaping. The spectrum of the incident femtosecond laser pulse was dispersed in space between a pair of diffraction gratings separated by a pair of lenses (see Fig. 1). A spatially resolved phase mask, which was located at dispersion plane, modified the Fourier transform of the incident pulse with computer control to produce a desired shape. The gratings with a groove number of 2400 lines/mm were used and the diffraction angle from the gratings was 73.7^o. A computer-addressable liquid-crystal spatial light modulator (LC-SLM) with 128 pixels was used as the phase mask. The resolution of the phase shift on LC-SLM was near 0.01π. The pulse shaper was located between the oscillator and the pulse stretcher to reduce the possibility of damage on the optics. The transmission of the laser power through the pulse shaper was about 60%. The incident laser pulse was shaped into a square-shaped pulse with phase-only filter by a numerical calculation, based generally on the intensity profile and the phase characteristics of the incident laser spectrum. To reduce the distortion and ripple on the temporal distribution of the shaped laser pulse, we reconstructed the pulse shape again by re-calculations using the shaped pulse spectra after the amplifier and the frequency conversion process.

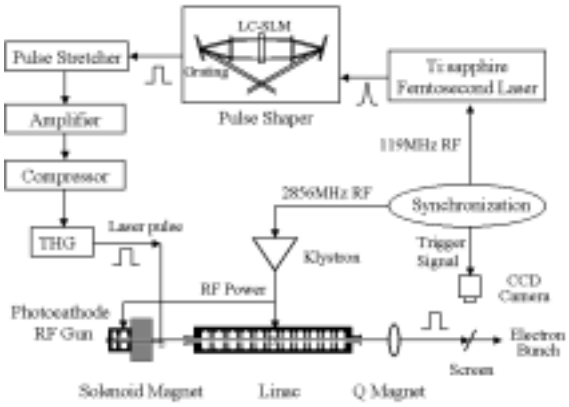

Figure 1: Experimental arrangement

The shaped pulse was stretched up to 150 ps in the pulse stretcher and amplified in the regenerative amplifier. The amplified pulse was compressed in the pulse compressor, and then frequency tripled to 266.7 nm UV light in a pair of nonlinear crystals. The UV light was injected onto the cathode surface at an angle of about 2° along the electron beam direction.

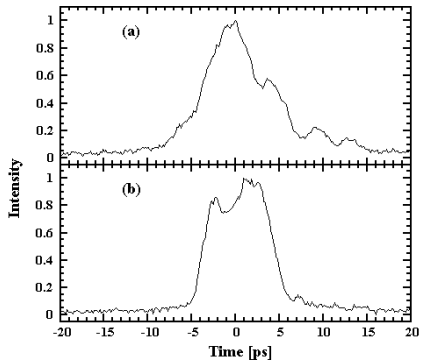

Figure 2: Temporal distributions of the Gaussian (a) and square (b) laser pulse shapes with a pulse length of 9 ps FWHM.

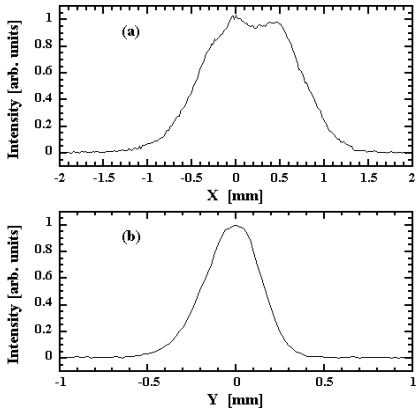

Figure 3: Spatial profiles of the laser beam in horizontal (a) and vertical (b) directions.

3 EXPERIMENTAL RESULTS

The typical Gaussian and square-shaped temporal distributions of the UV laser pulses with a pulse length of 9 ps FWHM are shown in Fig. 2. The data was measured by an X-ray streak camera with a time resolution of 2 ps, resulting a rise time of 1.5 ps for the square pulse shape. It is noted that the rise time of the actual pulse was less than 1.5 ps. The flatness of the square pulse reduced from 5% to 25% by lengthening the pulse from 4 to 14 ps FWHM. The pulse-to-pulse fluctuation of the shaped pulse length was about 7%. The spatial profile of the laser beam on the cathode is shown in Fig. 3. The beam spot size was 1.2 mm and 0.4 mm FWHM in the horizontal and vertical directions, respectively.

The normalized rms horizontal emittance measured as a function of the laser pulse length is shown in Fig. 4 for the Gaussian and square temporal pulse shapes. The electron bunch charge was fixed at 0.6 nC, and the solenoid field was set to 1.6 kG which was optimal for compensating the space charge emittance at 0.6 nC. The laser injection phase in the rf gun was 30° [6,7] and the rf phase of the linac was optimal to minimize the beam emittance. The data shows that the emittance increases at shorter and longer laser pulse length regions for both the Gaussian and square pulse shapes. This is behaved in

emittance growth due to space charge and rf effects: the space charge dominated for the short laser pulse, and the rf dominated for the longer laser pulse. An optimal emittance at 0.6 nC was indicated at laser pulse length of 8~10 ps FWHM. According to analytical studies [8], we fit the measured emittance as a function of

$$\varepsilon = \sqrt{(a/\sigma_l)^2 + (b\sigma_l^2)^2 + c^2}\ , \qquad (1)$$

where the first (second) term represents the linear space-charge (rf) induced emittance (assumed $\sigma_z \propto \sigma_l$, laser pulse length), a, b and c are parameters which are independent on the laser pulse length. The fits yield a=5.1±0.6, b=(7.3±0.9)x10^{-3} and c=0.44±0.22 for the square pulse shape, while a=9.1±1.3, b=(7.5±1.2)x10^{-3} and c=0.73± 0.28 for the Gaussian pulse shape. The parameters show that the square pulse shape reduced the linear space charge emittance of about 44% comparing with the Gaussian pulse shape, and a same rf induced emittance was observed for both the pulse shapes at a same pulse length. The parameter c in πmm-mrad represents thermal emittance and nonlinear space charge induced emittance which is not removed the emittance compensation process. The thermal emittance is independent on the pulse shape and should be a constant. Therefore, the fit indicates that the square pulse shape also reduced emittance growth due to the nonlinear space charge effect.

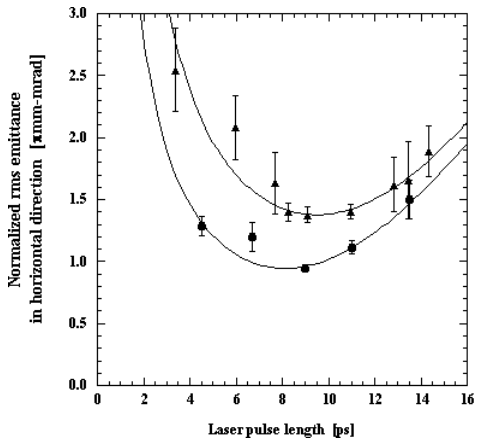

Figure 4: The emittance versus laser pulse length at 0.6 nC for the Gaussian (triangle) and square (dot) pulse shapes.

The normalized rms horizontal emittance was also measured as a function of the bunch charge for the Gaussian and square temporal pulse shapes with a pulse length of 9 ps FWHM, as shown in Fig. 5. The measured data was fit as a function of

$$\varepsilon = \sqrt{(a'Q)^2 + b'^2}\ , \qquad (2)$$

where a' is a fitting parameter referred to space charge force, and b' in πmm-mrad is a zero charge emittance. The fits yield a'=0.92±0.05 and b'=0.81±0.03 for the square pulse shape, while a'=1.85±0.13 and b'=0.83±0.05 for the Gaussian pulse shape. It is found that the square pulse shape reduced the space charge force of about 50% comparing with the Gaussian pulse shape, which is in a good agreement with the analysed results in Eq. 1.

However, the emittance measurements were made at the beam energy of 14 MeV, resulting in an emittance growth due to space charge effect in the drift region between the quadrupole and the screen. The emittance growth was estimated as <14% by PARMELA simulation under the experimental conditions. Another growth in emittance due to the given asymmetric laser beam was observed in the simulation as 22% comparing with the input of a symmetric laser beam at 1 nC.

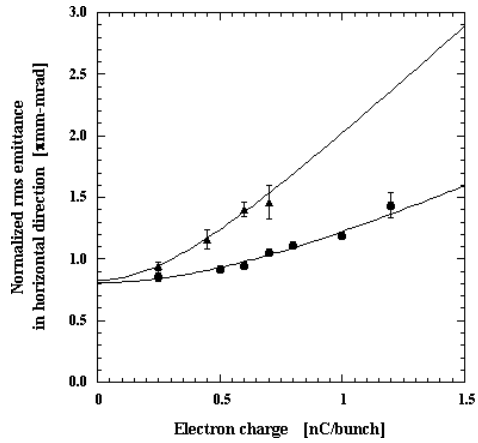

Figure 5: The emittance versus bunch charge for the Gaussian (triangle) and square (dot) pulse shapes at a pulse length of 9 ps FWHM.

4 CONCLUSSIONS

In summary, a technique of laser pulse shaping was developed and used to the low-emittance electron beam generation in the RF gun. The beam emittance was measured as functions of the laser pulse length and the bunch charge for both square and Gaussian temporal laser pulse shapes. An optimal normalized rms emittance of 1.2 πmm-mrad at 1 nC was obtained by a square temporal laser pulse shape with a pulse length of 9 ps FWHM.

This work was performed under the Femtosecond Technology Research Association (FESTA), supported by the New Energy and Industrial Technology Development Organization (NEDO).

5 REFERENCES

[1] M. Cornacchia et al., SLAC-R-521/UC-414, 1998.
[2] F. Richard et al., DESY Report 2001-011, 2001.
[3] J. Yang et al., Nucl. Instr. & Meth. A**428**, (1999) 556.
[4] L. Serafini et al., Phys. Rev. E **55**, (1997) 7565.
[5] M. Ferrario et al., Proc. of EPAC'2000, (2000)1642.
[6] F. Sakai et al., Jpn. J. Appl. Phys. **41**, (2002) 1589.
[7] J. Yang et al., Rev. Sci. Instr. **73**, (2002) 1752.
[8] K.-J. Kim, Nucl. Instr. Meth. A**275** (2000) 201.